

PCCP

Accepted Manuscript



This is an *Accepted Manuscript*, which has been through the Royal Society of Chemistry peer review process and has been accepted for publication.

Accepted Manuscripts are published online shortly after acceptance, before technical editing, formatting and proof reading. Using this free service, authors can make their results available to the community, in citable form, before we publish the edited article. We will replace this *Accepted Manuscript* with the edited and formatted *Advance Article* as soon as it is available.

You can find more information about *Accepted Manuscripts* in the [Information for Authors](#).

Please note that technical editing may introduce minor changes to the text and/or graphics, which may alter content. The journal's standard [Terms & Conditions](#) and the [Ethical guidelines](#) still apply. In no event shall the Royal Society of Chemistry be held responsible for any errors or omissions in this *Accepted Manuscript* or any consequences arising from the use of any information it contains.

In situ FTIR and Raman spectroelectrochemical characterization of graphene oxide upon electrochemical reduction in organic solvents

Cite this: DOI: 10.1039/x0xx00000x

Antti Viinikanoja^{*a}, Jussi Kauppila^{ab}, Pia Damlin^{*a}, Milla Suominen^a, Carita Kvarnström^{*a}

Received 00th January 2012,

Accepted 00th January 2012

DOI: 10.1039/x0xx00000x

www.rsc.org/

Electrochemical reduction of solution cast and self-assembled graphene oxide (GO) films on Au surfaces were studied using organic solvents. During the cyclic voltammetry measurements the structural changes in the films were recorded focusing on *in situ* infrared and Raman techniques. Both FT-Raman and dispersive Raman spectroscopy were utilized for the reduction studies. The spectroelectrochemical results indicate that the changes in the GO structure takes place in a quite narrow potential range extending from -1 to -1.7 V. Higher negative potentials gives rise to reversible changes in the spectra and are not due to reduction processes of GO but more related to changes in the electrolyte media.

Introduction

Graphene, a two-dimensional nanostructured carbon material, has attracted extensive interest since its discovery in 2004.^{1,2} It promises exciting potential applications in various fields, such as supercapacitors,^{3,4} batteries,⁵ nanocomposite materials^{6,7} and sensors.^{8,9} There are many approaches to the preparation of graphene and the most commonly used methods include mechanical exfoliation,¹ chemical vapor deposition¹⁰ and chemical/electrochemical reduction of graphene oxide (GO).^{11,12,13} The synthesis route from GO is considered to be the most economical way for mass production of graphene. The oxidation results in graphite sheets heavily decorated by oxygen-containing groups both in- and out-of-plane of the graphitic layer, which not only expand the interlayer distance but also make the product hydrophilic.¹⁴ A lot of effort has recently been put into searching for ways to treat the chemically oxidized graphite and how to restore the original structure of graphene and its exceptional properties. The available and most explored methods include thermal treatment,¹⁵ chemical reduction using hydrazine or other reductants,^{11,16} plasma¹⁷ and electrochemical reduction.^{12,13,18,19} But so far none of the presented methods is able to fully heal the defects caused by oxidation.

The electrochemical reduction method has been introduced as a fast and environmentally friendly way for producing a partly recovered sp² lattice. Compared to all of the GO reduction methods mentioned above, the mechanism of GO reduction by electrochemical means is the least understood at the moment. While electrochemistry alone cannot tell details about structural changes in thin films it is often applied in combination with a spectroscopic technique.^{20,21} We have previously used surface sensitive IR techniques to follow the evolution of oxygen containing defects upon electrochemical reduction of self-assembled films of graphene oxide in aqueous solutions²² and also reported on the completeness and differences observed in the structure of electrochemically reduced GO (rGO) films when going from one electrolyte media to another.¹² In this study, we examined spectral changes occurring when graphene oxide

was electrochemically reduced in a few common organic solvents using both *in-situ* FTIR and Raman spectroscopy techniques. Organic solvents, acetonitrile (AN), propylene carbonate (PC), and tetrahydrofuran (THF), were selected due to their broad electrochemical potential window. The change of electrolyte from water to organic media allows us in this work to extend the negative potential range used for the reduction of GO. Raman spectroscopy is an efficient method to identify and characterize various carbon nanostructures, while IR-spectroscopy gives information about the presence of oxygen-containing functional groups. The combination of these techniques gives the possibility to compare the potential induced changes in the oxygen-containing functional groups, as well as reorganization in the GO nanostructure as the electrochemical reduction of GO progresses. In contrast to our previous paper,¹² in which we looked at rGO by *ex-situ* techniques, we are now able to obtain detailed information on the gradual structural changes taking place in the GO film as the reduction potential is made more cathodic. In this work, single reflection FTIR spectroscopy in Kretschmann-ATR configuration and Raman spectroscopy, both in FT-Raman and in dispersive mode were used to characterize the rGO film. Measurements using the surface enhanced Raman spectroscopy (SERS) technique were carried out on thin self-assembled GO films, so that the results would be comparable to our previous results obtained in aqueous solutions.²² The results indicate that the electrochemical reduction of GO films simultaneously lead to gradual changes in the GO nanostructure and to removal of oxygen-containing functional groups from the surface. The potential range, where the reduction related structural changes of GO were observed was dependent on the solvent used.

Experimental

Materials

Anhydrous acetonitrile (Sigma-Aldrich) and tetrahydrofuran (>99.9 %, inhibitor-free, Sigma-Aldrich), LiPF₆ (Sigma-Aldrich), 2-mercaptoethylamine (MEA) (Sigma-Aldrich) and

ferrocene (Sigma-Aldrich) were used as received. Propylene carbonate (Merck) was vacuum-distilled and stored over molecular sieves prior to use. All solvents and electrolytes were stored in an argon filled glove box. Graphene oxide was synthesized from natural graphite flakes (Alfa Aesar, mesh 325, 99.8 %) according to a modified Hummers method²³ and purified by centrifugation and dialysis.

Methods and characterization

Electrochemistry. All electrochemical and spectroelectrochemical measurements were conducted using a three electrode configuration with PGSTAT101 (Autolab), Iviumstat (Ivium) and 263A (EG&G Instruments) as potentiostats. The three-electrode system consists of a gold working electrode, platinum counter electrode and Ag/AgCl quasi reference electrode. The quasi reference electrode was tested against ferrocene before and after measurements. In cyclic voltammetric measurements the working electrode diameter was 2.0 mm. Samples were prepared by drop casting 5 μL ($c_{\text{GO}} = 0.5 \text{ mg/mL}$) of GO solution onto the gold electrode. Electrolyte solutions of 0.1 M LiPF_6 in acetonitrile, tetrahydrofuran and propylene carbonate were prepared in argon filled glove box prior to use.

Raman. Surface enhancement effect for FT-Raman spectroscopy was achieved by electrochemically roughening of a gold electrode (2.0 mm diam., CHI Instruments Inc. CHI101).²⁴ Raman measurements were done using Nexus 870 FTIR spectrometer (Nicolet) equipped with a Raman accessory. A more detailed description of the used in situ Raman technique has been published elsewhere.²² Wavelength of the used Raman laser was 1064 nm and all spectra were recorded by collecting 128 scans with a 4 cm^{-1} spectral resolution. The roughened gold electrode was coated with a monolayer of 2-mercaptoethylamine (10 mM aqueous solution for an hour) in order to create a positively charged electrode surface. A GO monolayer was applied on the electrode through self-assembly by dipping the working electrode in GO solution ($c_{\text{m}}=0.25 \text{ mg/mL}$, pH adjusted to 1.5 with H_2SO_4) for two hours. The dispersive Raman measurements were made from drop cast GO films on Au electrode. A flow through electrochemical cell was used for the in situ measurements and has been described in detail in an earlier work.²⁵ Raman experiments with visible laser excitation were performed with a Renishaw Ramascope (system 1000 B) equipped with a Leica MLM microscope and connected to a thermoelectrically cooled charged-coupled device (CCD) detector. The excitation wavelength for the Raman scattering was provided by an argon laser with excitation wavelength of 514 nm (LaserPhysics) using a laser power of 10 mW. The scattering signal was obtained at 90 degrees angle to the excitation beam. Calibration of the spectrometer was performed before the measurements using a Si standard.

IR. In situ IR measurements were done using the same Nexus 870 FTIR spectrometer as stated above, equipped with SeagullTM variable angle reflection accessory (Harrick). An in-house built flow through electrochemical cell with a gold covered 12.5 mm radius hemisphere ZnSe crystal was attached to measurement bench (see supplementary information FS1 and FS2 for more details). The measurement cell uses Kretschmann configuration with a 45 degree angle of incidence. Typically 128 scans were recorded with a 4 cm^{-1} spectral resolution.

Samples were prepared by drop casting 60 μL ($c_{\text{GO}} = 2 \text{ mg/mL}$) of GO on top of the gold covered ZnSe crystal on an area of roughly 5 mm in diameter.

Spectroelectrochemistry. In IR and Raman spectroelectrochemical measurements stepwise increasing negative potentials between 0 and -2.5 V were applied to the cell for 4 or 5 minutes, respectively. At each potential the material was allowed to stabilize for two minutes before recording the spectra. Absorbance spectra were obtained using the single beam spectrum measured at initial potential as a background. The transformation and correction of a possible small drift in absorbance spectra were done using Origin 8.0 software.

Results and Discussion

Characterization and assembly of GO nanosheets

Water-soluble GO nanosheets prepared according to a modified Hummers method²³ were characterized with atomic force microscopy (AFM) (FS3 in the electronic supplementary material). The AFM image shows that the self-assembled GO films consist of well dispersed wrinkled and folded flakes with a thickness below 3 nm. The step height of the self-assembled GO films, obtained by analysis of the AFM cross-sectional profile, is about 1.1 nm, which is consistent with previous reports, suggesting the single-sheet nature of GO in this work.^{12,22,26} On the other hand, the drop casted GO films are considerably thicker, showing an average thickness of 97 nm. According to SEM images, these films were smooth with some scaly structures and retained their morphology after reduction.¹² The amine groups in MEA possess a pK_a value of 7.6.²⁷ As the pH of the as-prepared GO solution is 2.5 the amine groups on a MEA primed gold surface are mainly in protonated form making the surface positively charged. The assembly process of negatively charged GO sheets on a MEA primed gold surface was followed by surface plasmon resonance and AFM measurements²² and the optimized conditions found was used also in this work (adsorption time of 240 min, $c_{\text{GO}} = 1 \text{ mg/mL}$ and a pH of 2.5).

Electrochemical characterization of GO upon reduction in acetonitrile

Electrochemistry offers an effective tool for modification of electronic states by adjusting the external potential source to change the Fermi energy level of the electrode material surface. It has been proven to be a simple, fast, efficient, low-cost, and environmentally friendly way for the reduction of GO films.^{12,13,18,19} The electrochemical reduction of a drop casted GO film on a gold electrode in acetonitrile is shown in Figure 1. The cyclic voltammogram shows that reduction of GO starts at -1.0 V with a peak current maximum at -1.8 V. The reduction is found to be irreversible showing no oxidation peak in the reverse scan. It also seems to be completed in a single scan as no reduction peak currents are observed in subsequent cycles. The quite broad potential range observed is typical for GO materials containing different oxygen functional groups.²⁸ In this process, various oxygen groups, including -OH, -COOH, and epoxides are reduced.^{29,30} Recently, the carboxylic acid groups on GO has been shown to be more stable against moderate reduction potentials than the other functional groups that are reduced already at ca. -1 V (vs.

Ag/AgCl).³¹ In a previous work using ex situ spectroscopic analysis we showed that several reduction reactions take place at potentials even after the potential where the current peak is visible in the cyclic voltammograms.¹²

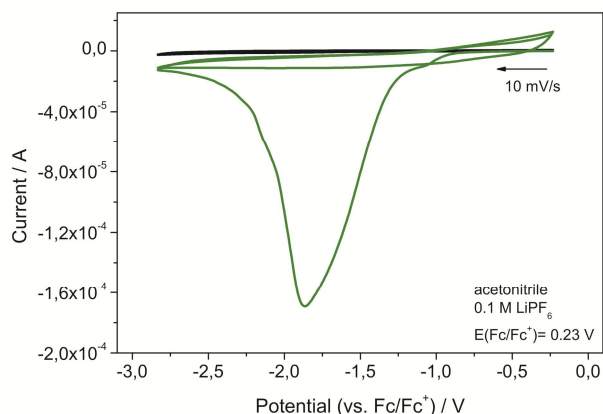


Figure 1. Cyclic voltammogram (CV) of a drop casted GO film on top of a gold covered ZnSe reflection element in 0.1 M LiPF₆ (AN) with a scan rate of 10 mV/s. The arrow indicates the sweep direction and the black line shows the response obtained for the bare Au electrode in the same electrolyte.

In situ spectroelectrochemical characterization of GO upon reduction

FTIR spectroscopy in the Kretschmann-ATR configuration.

In an earlier work we studied the electrochemical reduction of a few layers of GO deposited by self-assembly on a roughened gold plated silicon reflection element in aqueous media.²² The results showed that the effect of the applied potential on the GO structure could be divided into two parts where the changes occurring at moderate negative potentials (0 to -0.8 V) are mainly related to changes in the double layer at the film-electrolyte interface and to hydrogen bonding of intercalated water between the GO sheets. At potentials more negative than -0.8 V vs. Ag/AgCl the reduction of GO started to take place with concomitant conversion of the different functional groups of the film. Using the Attenuated Total Reflection (ATR) geometry i.e. entering the film from the backside through the reflection element we could minimize the interference from

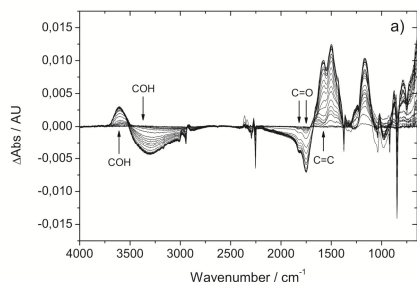


Figure 2a. In situ FTIR difference spectra recorded during electrochemical reduction of GO in 0.1 M LiPF₆/AN (measurement time in total 96 min). The spectra gathered at constant potentials every 0.1 V in the potential range -0.3 to -2.6 V are shown. The spectrum at -0.2 V (vs. Fc/Fc⁺) is used as reference.

electrolyte contribution to the spectra and get the main signal from intercalated water and the potential dependent change of the functional groups in GO. In this work we also use the reflection Fourier Transform Infrared Spectroscopy technique but now in the Kretschmann geometry.³² This technique requires the use of a thin metal film deposited on an internal reflection element (IRE) in order for the electric field to pass through the metal film. ZnSe elements with a thin layer of gold were produced by vacuum evaporation. The changes observed in the IR spectra at the spectral range 1000-4000 cm⁻¹, as the potential is increased towards more cathodic values are shown in Figure 2a. In this experiment AN was used as organic solvent and the focus is put onto the changes taking place in the potential range between -0.5 to -1.7 V (Fc/Fc⁺). This potential range was chosen according to the CV in Figure 1, a significant increase in the reduction current could be observed in this particular potential range. As the potential induced changes in absorbance are plotted in relation to the initially applied potential, the upward extending peaks will indicate the gain and the downward extending peaks the loss of structural rearrangements and functional groups in GO during electrochemical reduction. In the range of 3700-3100 cm⁻¹ overlapping C-OH modes, originating from a wide range of functional groups on the GO sheets, gives rise to a broad spectral response. Within this range at least the following four main vibrations can be distinguished. At 3200 (overtone of scissor vibrations of adsorbed water molecules), 3370 (closely neighboring hydroxyl groups), 3500 (carboxyl groups of GO), and the one at 3625 cm⁻¹ (C-OH stretch associated to five-membered-ring lactols and hydroxyl groups of GO from both the basal plane and from the sheet edges).^{33,34} The GO film also gives rise to well documented vibrations in the lower wavenumber region as the band at 1750 cm⁻¹ with a shoulder at 1820 cm⁻¹ from the C=O stretching vibrations of carbonyl and ketonic species. In the range around 1600 cm⁻¹ overlapping bands from OH bending of water (1620 cm⁻¹) and asymmetric vibrational C=C stretching of sp²-hybridized carbons (1579 cm⁻¹) can be observed. The continuously increasing negative peak at 847 cm⁻¹ is due to the electrolyte salt PF₆⁻ being expelled from the vicinity of the electrode upon the reduction reaction. As AN only shows a major peak at 1180 cm⁻¹ it is well suited for monitoring the GO reduction and does not overlap with any of the vibrations related to the reduction of GO. The plot in

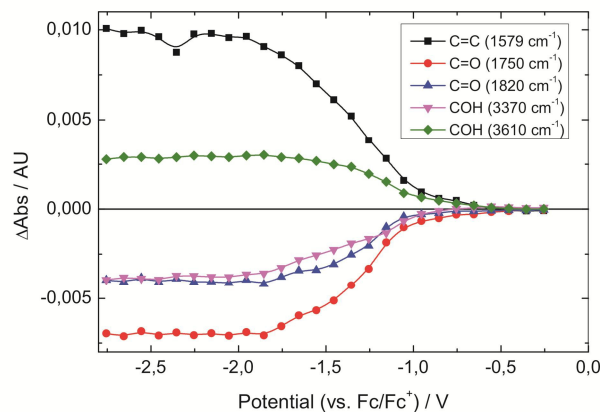


Figure 2b. The intensity dependence of GO related vibrational bands on the applied potential during the reduction process using the spectrum measured at -0.2 V as reference spectra.

Figure 2b follows the change in absorbance for some of the aforementioned bands with reduction potential using the

absorbance obtained at -0.2 V as reference point. As can be seen from the plot, the reduction of GO and subsequent conversion of the functional groups is clearly observed at potentials more negative than -0.5 V. From this potential onwards to -1.8 V a continuous increase in bands at 1579 and 3610 cm^{-1} and furthermore decrease of the bands at 1750, 1820 and 3370 cm^{-1} can be found. All of these spectral changes indicate clearly reconstruction of the graphitic domains and subsequent loss of oxygen containing functional groups. The reason for increase in absorbance intensity at 3610 cm^{-1} can be explained by formation of hydroxyl groups -C-OH originating from the reduction of the epoxides and carboxyl groups. Overall the changes obtained in the IR spectra coincide nicely with the charge consumed during the spectroelectrochemical measurement (Fig. 2c). While the absorbance intensity stays more or less constant the residual capacitive contribution on charge curve cause the small slope observed after -1.8 V. Moreover, from fig. 2a it can clearly be observed that when using potentials more negative than -1.8 V for the reduction of GO only minor changes in intensity of all the vibration modes takes place reaching more of a steady state situation.

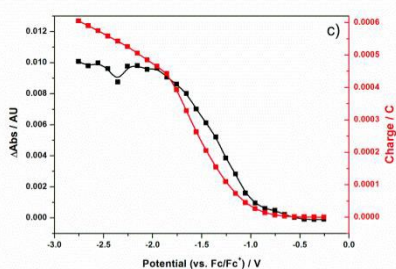


Figure 2c. Changes in the intensity of GO related C=C vibrational band at 1579 cm^{-1} and the charge consumed during the in situ spectroelectrochemical experiment (from -0.2 to -2.7 V).

Also THF and PC was used as organic solvents for the in situ study of the reduction process of GO. The difference spectra

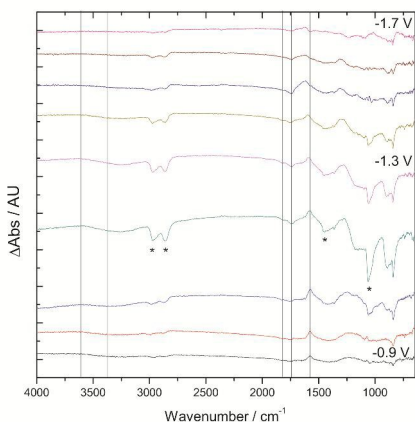


Figure 3. In situ FTIR spectra recorded during electrochemical reduction of GO in 0.1 M LiPF_6 in THF. The spectra are shifted for clarity and only spectra in the potential range -0.9 to -1.7 V are shown. The absorbance related to previous applied potential is used as reference. The strong negative peaks at 2970, 2860, 1440, 1064 cm^{-1} are due to the solvent THF and marked by an asterisk.

obtained using THF are shown in Figure 3. In the spectra the solvent peaks are marked with asterisk (*). Unfortunately, in the case of PC there was a strong overlapping of peaks related

to the solvent (1670, 1780, 1300 and 1200 cm^{-1}) and to the reduction of GO making it impossible to quantify the effect of reduction of GO from absorbance intensities. However, this solvent was well suited for in situ Raman measurements and was therefore used also in IR measurements as comparison (shown as FS4 in the electronic supplementary material). It should be pointed out that THF is known to decompose at high negative potentials (> -2.2 V), especially when combined with lithium ions, causing further problems in electrochemistry and for spectral interpretations.³⁵ In these two media the main spectral changes observed follows along the lines already discussed above using AN as solvent system. However, the potential where changes starts to be prominent are slightly shifted to -1.2 V (vs. Fc/Fc^+). Also when using PC and THF the main changes coincides well with the potential range where a significant increase and finally a fairly constant level in the reduction current is reached in the CVs (-1 to -1.7 V).

Raman spectroscopy (surface enhanced FT-Raman and dispersive). Raman spectroscopy provides a sensitive and gentle characterization tool for graphene and nanocarbon materials in general. It can distinguish between single-layer, bilayer, and multilayer graphene, and is also highly sensitive to the electronic structure of these materials.³⁶ In graphene oxide the information is additionally provided on the defect density and crystallite size.³⁷ The important features observed in the Raman spectra are the G mode and the G' mode, also sometimes referred to as the 2D mode.³⁸ These G and G' modes are present in all graphene-based materials but their frequencies, intensities, and line widths are influenced by a number of factors such as number of graphene layers, the external/intentional doping or unintentional doping, stress, and the laser excitation energy. In some graphene samples, the D line is also found and the D line is believed to indicate the presence of defects as in ordinary graphite.³⁹

Quantifying defects in graphene related systems, which include a large family of sp^2 carbon structures, is crucial both to gain insight in their fundamental properties and for applications. In graphene this is a key step toward the understanding of the limits to its ultimate mobility. Significant efforts have been devoted to quantify defects and disorder using Raman spectroscopy for nanographites, amorphous carbons, carbon nanotubes, and graphene. The first attempt was the pioneering work of Tuinstra and Koenig.⁴⁰ They reported the Raman spectrum of graphite and nanocrystalline graphite and assigned the mode at ~ 1580 cm^{-1} to the high frequency E_{2g} Raman allowed optical phonon, now known as G band.⁴¹ In defect and nanocrystalline samples they measured a second peak at ~ 1350 cm^{-1} , now known as D band. It was assigned to an A_{1g} breathing mode at the Brillouin Zone boundary K, activated by the relaxation of the Raman fundamental selection rule $q \approx 0$, where q is the phonon wavevector.⁴⁰ They noted that the ratio of the D to G intensities varied inversely with the crystallite size, L_a .

As was already discussed in ref. 22, the redox reactions of the different oxygen containing functional groups in GO lie very close to each other. This makes a complete identification of all groups in an in situ Raman measurement in aqueous electrolyte solutions impossible. In order to obtain deeper insight into the reduction process of GO, in situ Raman measurements were in this work conducted using different organic solvents. Before reduction the self-assembled GO films on MEA modified rough gold surface were analyzed by surface enhanced Raman spectroscopy in the same solvent systems as used for the IR

measurements (AN, PC, or THF). In Fig. 4, the characteristic

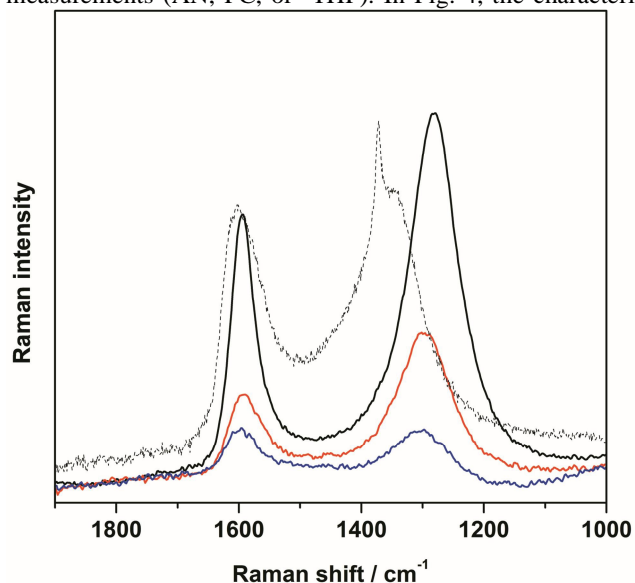


Figure 4. Raman spectrum of GO film on Au at $-0.2/-0.4$ V (vs. Fc/Fc^+) in AN (black), PC (red), and THF (blue) using both the FT-Raman and dispersive technique. The dashed line represents the measurement in AN at 514 nm laser excitation.

Raman features of graphene oxide are observed with 1064 nm laser excitation wavelength showing a broad and intense D band at ~ 1300 cm^{-1} and overlapping G and D' (not discernible) bands at ~ 1600 cm^{-1} . The G' (or 2D), $\text{D}+\text{D}'$ and 2G bands at ~ 2580 , ~ 2920 , and ~ 3200 cm^{-1} are shown as supplementary FS5. Additionally, $\nu(\text{CH})$, $\nu(\text{CN})$, $\nu(\text{CC})$ vibrations of electrolytes (AN, PC, THF) are observable.

For comparison, Raman measurements in AN from a drop casted film on gold electrode using a dispersive Raman instrument with excitation wavelength at 514 nm are also shown in Fig. 4 (dashed line). As can be seen, the dispersive nature of D and G' modes cause the frequency to shift as function of the energy of the incident laser. However, also the position of G mode (actually $\text{G}+\text{D}'$) is slightly shifted, that can be explained by the different intensity and band width contribution of dispersive D' feature to this combination band at different excitation wavelengths that shift the apparent position of the band.

The Raman spectra in Fig. 5 obtained in situ during gradual electrochemical reduction in AN, PC and THF were fitted in the range $1900 - 1000$ cm^{-1} in order to follow the subtle changes occurring in G and D bands during the electrochemical reduction of a GO film on a gold electrode. According to earlier reports the D band was fitted by a Lorentzian shape and the G band ($\text{G}+\text{D}'$) was treated as an asymmetric band approximated with Breit-Wigner-Fano lineshape.^{42,43} Based on these results a clear evidence about progressive reduction of graphene oxide is obtained in all three organic solvents studied. We focused on the change of G and D band positions, linewidths, intensities (I_{D} , I_{G}), and the $I_{\text{D}}/I_{\text{G}}$ -ratio. Out of these, the $I_{\text{D}}/I_{\text{G}}$ -ratio increase has generally been used as a measure for the extent of GO reduction when using different reduction methods, including electrochemical reduction.^{7,22} Ferrari and Robertson introduced a three-stage model that relates the $I_{\text{D}}/I_{\text{G}}$ -ratio

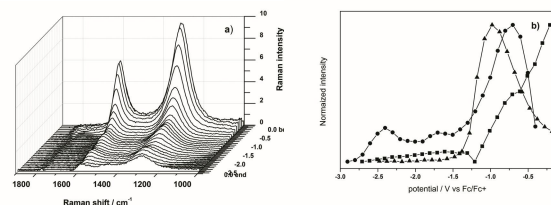


Figure 5. (a) The evolution of G and D bands as a function of potential during the electrochemical reduction of the self-assembled monolayer on gold electrode in propylene carbonate. (b) The intensity of G band as a function of the applied potential in AN (■), PC (●), and THF (▲).

increase to structural ordering of graphene based materials.^{43,44} Linewidth narrowing together with G band shift has been used recently to follow the structural ordering during the reduction process of graphene oxide.⁴⁵ In Fig. 6, the evolution of G band

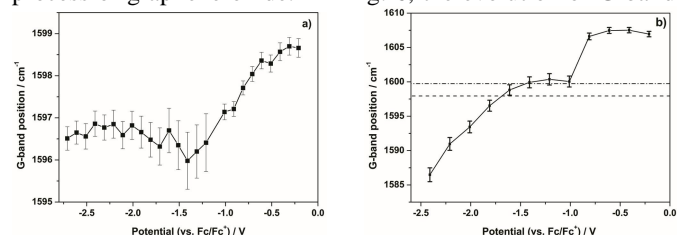


Figure 6. Changes in G band position during in situ electrochemical reduction of GO in acetonitrile. SERS (a) measurements (FT-Raman, $\lambda_{\text{ex}} = 1064$ nm) on a single layer GO and dispersive (b) Raman measurements (dispersive Raman, $\lambda_{\text{ex}} = 514$ nm) on thin GO film. The horizontal lines in (b) indicate the G band position at -0.2 V (---), and without (- -) applied potential. (0.1 M LiPF_6 in acetonitrile, W: Au, Ref.: Ag/AgCl , Aux.: Pt)

position as a function of applied potential is presented at both laser excitation wavelengths (1064 and 514 nm). In AN it is clearly seen that the G band downshifts from 1599 to 1596 cm^{-1} as the electrochemical reduction of the GO monolayer under 1064 nm laser excitation progresses. The change in G band position at visible excitation follows the same trend as above but shows considerably stronger shift. Here the G band position shifts from 1607 cm^{-1} to 1586 cm^{-1} in the potential range ($-0.2 \rightarrow -2.7/-2.4$ V vs. Fc/Fc^+). In the literature, there are some inconsistencies about the direction of the G band shift during the reduction process and it is suggested that shape and intensity alternations of D' band within the G band are mainly responsible for this behavior.^{27,43,45} The changes in G band position does not progress steadily as function of applied potential, but shows an abrupt downshift in the potential range -0.8 to -0.9 V (vs. Fc/Fc^+) (seen more clearly under visible laser excitation). This is well before the main reduction peak (at -1.86 V vs. Fc/Fc^+) for a GO monolayer in AN can be observed when looking at the cyclic voltammogram in Fig. 1. However, the onset of this reduction peak at -1.25 V and small pre-peak at ca. -1.0 V might be related to this abrupt change in the G band position. After -0.9 V the position of G band remains constant in a moderate negative potential range down to ca. -1.5 V (vs. Fc/Fc^+) (taking into account the error limits). After -1.5 V the G band position remain unchanged under 1064 nm laser excitation, but under visible excitation the G band shifts further down as the potential is made more negative. However, this downshift in band position is reversible in contrary to the behavior of the position for the G band obtained before -1.5 V

(vs. Fc/Fc^+), which is irreversible. The irreversibility of the process occurring in GO is realized upon applying open circuit condition or the starting potential, 0.0 V (vs. Fc/Fc^+), after electrochemical reduction and measuring the Raman spectrum. Using the aforementioned fitting procedure for the bands, the G band position remains at the level obtained between the potentials -1.0 - -1.5 V (vs. Fc/Fc^+) during the reduction process (shown as horizontal lines in Fig. 6). The Raman results agree well with the irreversible electrochemical reduction of the GO film observed under cyclic voltammetry experiments and also with previously published results.^{12,45} The potential ranges where changes can be observed in the spectra also coincide nicely with those obtained using the in situ IR technique.

The reduction process of a self-assembled GO film on rough Au-surface was followed by SERS in PC similarly as in case of AN. Fig. 7 presents the evolution of the G band position as function of applied potential in the potential range -0.4 V to -2.9 V (vs. Fc/Fc^+). Also in this case a downshift of the G band during the reduction process of GO is obvious. However, instead of one abrupt change in band position as in AN, the shift in band position takes place within two potential regions in PC, -0.9 - -1.3 and -1.8 - -2.0 V (vs. Fc/Fc^+) (Fig. 7). After the reduction process the G band position returns back to values obtained in the potential range between -2.0 and -2.5 V (vs. Fc/Fc^+), resembling the behavior in AN (-1.0 - -1.5 V vs. Fc/Fc^+). In AN and PC, the changes observed in D mode position closely follow the changes of the G mode in the irreversible part of the reduction process.

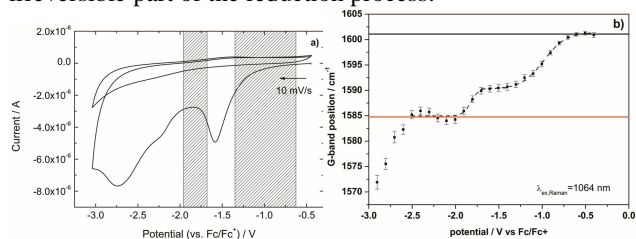


Figure 7. Cyclic voltammometry of self-assembled monolayer of GO on rough Au electrode in PC/LiPF₆ (a) and shift in G band position during the reduction process (b). The shaded areas in (a) mark the potential region where 90 % of G band shift (b) occurs. The horizontal lines in (b) indicate the G band position before (**black**) and after (**red**) the reduction of GO film without an applied potential and at -0.4 V (vs. Fc/Fc^+).

Cyclic voltammometry of the self-assembled monolayer on gold in Fig. 7 show several processes taking place during the electrochemical reduction of GO in PC. Because of the different timescale of the experiments (kinetic control in CV vs steady state in Raman), reduction peaks in the voltammogram are shifted towards more cathodic potentials with respect to the processes seen in SERS.

Raman observations can also be related to changes observed during the in situ IR measurements. As already shown in Fig. 2b C=O, C=C, and C-OH stretching bands can be easily used to follow the progress of electrochemical reduction of GO. The conversion of oxygen containing functionalities starts when potentials more negative than -0.5 V (vs. Fc/Fc^+) are applied, that coincides well with first weak G band shifts in AN and first faradaic processes observed in the cyclic voltammometry of GO monolayer indicating clearly that origin of all above changes are related to GO monolayer reconstruction under applied potential. From this potential onwards to -1.6 V a continuous increase in bands at 1579 and 3610 cm^{-1} and furthermore

decrease of the bands at 1750, 1820 and 3370 cm^{-1} can be found. The potential range, where the strongest changes occur are somewhat shifted when the IR and Raman measurements are compared with each other. As we have shown earlier, the thickness of the GO film can affect the observed reduction potential.¹² In this case thicker films needed for IR measurements shift processes to slightly more cathodic potentials; also the different origin of the vibrations, sp^2 hybridized carbon (Raman) vs functional groups on the basal plane of GO (IR) can have some effect.

Raman results in aqueous solutions are shown as comparison in supplementary FS6 using the same fitting procedure for the G- and D-bands (as above).²² To facilitate comparison to our earlier results it is assumed that the potential of Ag/AgCl-reference electrode vs. Fc/Fc^+ -couple is ca. -0.44 V (+0.197 V Ag/AgCl vs. NHE and +0.64 V Fc/Fc^+ vs. NHE). As in organic solvents, the minimum in the G-band position is obtained at ca. -1.0 V (vs. Fc/Fc^+) after which the position of the band remains constant as more negative potentials are applied. Interestingly, the response is different when the applied potential is set back to its initial value. For the GO film reduced in aqueous solutions the G-band position is higher than the value obtained in organic solvents (compared to a plateau in band position in Figs. 6b, 7b, and FS6). This indicates that the reduction process of the GO film is more efficient in AN and PC than in aqueous solutions.

Conclusions

Self-assembled and solution cast films of GO have been prepared and characterized focusing on in situ spectroelectrochemical techniques. The electrochemical and spectroelectrochemical behavior of GO films during the electrochemical reduction in organic solvents showed similar but not the same changes to that of GO films in aqueous media. Obtained results clearly indicate that the electrochemical reduction of GO is more effective in organic than in aqueous solutions. According to the spectroelectrochemical results obtained upon the reduction of a GO film we can state that this process can be controlled by the choice of reduction potential and electrolyte medium. At potentials more negative than -0.5 V the reconstruction of graphitic domains is evident based on in situ IR measurements. The G band is a collective vibration corresponding to the aromatic domains in GO located in the basal plane. Concurrently with changes in IR, the in situ Raman spectroscopy clearly shows shift in G band position. This irreversible shift in the G band position result from chemical changes, i.e., irreversible removal of functional groups within or close to the aromatic domains in GO. According to the in situ IR and Raman measurements, the GO reduction does not significantly proceed at potentials more cathodic than ca -1.5- -1.8 V in acetonitrile. The reversible shift of the G band at highly cathodic potentials can be attributed to the charging of the conducting material and to the adsorption-desorption of solvent or electrolytes on the RGO sheets. The reduction in THF and PC follows a similar path showing a leveling of the G band position although a bit shifted to more cathodic potentials. Furthermore, in PC two potential regions can be observed for the shift in the band position.

Acknowledgements

The financial aid from the Academy of Finland, and the Magnus Ehrnrooth foundation is gratefully acknowledged.

Notes and references

^aTurku University Centre for Materials and Surfaces (MATSURF), Laboratory of Materials Chemistry and Chemical Analysis, University of Turku, 20014 Turku, Finland, E-mail: viinikan@utu.fi, pia.damlin@utu.fi, carkva@utu.fi; Fax: +358 2 333 6700; Tel.: +358 2 333 6714, Tel.: +358 2 333 6713, +358 2 333 6729

^bThe Finnish National Doctoral Programme in Nanoscience (NGS-NANO), Nanoscience Center, P.O. Box 35, 40014, University of Jyväskylä, Finland

Electronic Supplementary Information (ESI) available: Preparation and schematics of the ZnSe element used as working electrode for the IR spectroelectrochemical measurements, additional *in situ* FTIR and Raman spectra of GO film in AN, PC, and THF, AFM image of self-assembled GO film, and figures showing the G-band evolution in aqueous solutions and D-band evolution under visible excitation. See DOI: 10.1039/b000000x/

- K. Novoselov, A. Geim, S. Morozov, D. Jiang, Y. Zhang, S. Dubonos, I. Grigorieva and A. Firsov, *Science*, 2004, **306**, 666-669 (DOI:10.1126/science.1102896)
- F. Schedin, A. K. Geim, S. V. Morozov, E. W. Hill, P. Blake, M. I. Katsnelson and K. S. Novoselov, *Nat. Mater.*, 2007, **6**, 652-655 (DOI:10.1038/nmat1967)
- X. Cao, Y. Shi, W. Shi, G. Lu, X. Huang, Q. Yan, Q. Zhang and H. Zhang, *Small*, 2011, **7**, 3163-3168 (DOI:10.1002/sml.201100990)
- X. Dong, H. Xu, X. Wang, Y. Huang, M. B. Chan-Park, H. Zhang, L. Wang, W. Huang and P. Chen, *Acs Nano*, 2012, **6**, 3206-3213 (DOI:10.1021/nn300097q)
- M. Liang and L. Zhi, *J. Mater. Chem.*, 2009, **19**, 5871-5878 (DOI:10.1039/b901551e)
- T. Ramanathan, A. A. Abdala, S. Stankovich, D. A. Dikin, M. Herrera-Alonso, R. D. Piner, D. H. Adamson, H. C. Schniepp, X. Chen, R. S. Ruoff, S. T. Nguyen, I. A. Aksay, R. K. Prud'homme and L. C. Brinson, *Nature Nanotechnology*, 2008, **3**, 327-331 (DOI:10.1038/nnano.2008.96)
- X. Huang, S. Li, Y. Huang, S. Wu, X. Zhou, S. Li, C. L. Gan, F. Boey, C. A. Mirkin and H. Zhang, *Nature Communications*, 2011, **2**, 292 (DOI:10.1038/ncomms1291)
- L. Wang, K. Pu, J. Li, X. Qi, H. Li, H. Zhang, C. Fan and B. Liu, *Adv Mater*, 2011, **23**, 4386-+ (DOI:10.1002/adma.201102227)
- Y. Liu, X. Dong and P. Chen, *Chem. Soc. Rev.*, 2012, **41**, 2283-2307 (DOI:10.1039/c1cs15270j)
- A. Reina, X. Jia, J. Ho, D. Nezich, H. Son, V. Bulovic, M. S. Dresselhaus and J. Kong, *Nano Letters*, 2009, **9**, 30-35 (DOI:10.1021/nl801827v)
- D. R. Dreyer, S. Park, C. W. Bielawski and R. S. Ruoff, *Chem. Soc. Rev.*, 2010, **39**, 228-240 (DOI:10.1039/b917103g)
- J. Kauppila, P. Kunnas, P. Damlin, A. Viinikanoja and C. Kvarnstrom, *Electrochim. Acta*, 2013, **89**, 84-89 (DOI:10.1016/j.electacta.2012.10.153)
- A. Ambrosi, C. K. Chua, A. Bonanni and M. Pumera, *Chem. Rev.*, 2014, **114**, 7150-7188 (DOI:10.1021/cr500023c [doi])
- S. Stankovich, D. A. Dikin, G. H. B. Dommett, K. M. Kohlhaas, E. J. Zimney, E. A. Stach, R. D. Piner, S. T. Nguyen and R. S. Ruoff, *Nature*, 2006, **442**, 282-286 (DOI:10.1038/nature04969)
- C. Mattevi, G. Eda, S. Agnoli, S. Miller, K. A. Mkhoyan, O. Celik, D. Mastrogiovanni, G. Granozzi, E. Garfunkel and M. Chhowalla, *Advanced Functional Materials*, 2009, **19**, 2577-2583 (DOI:10.1002/adfm.200900166)
- H. A. Becerril, J. Mao, Z. Liu, R. M. Stoltenberg, Z. Bao and Y. Chen, *Acs Nano*, 2008, **2**, 463-470 (DOI:10.1021/nn700375n)
- C. Gomez-Navarro, R. T. Weitz, A. M. Bittner, M. Scolari, A. Mews, M. Burghard and K. Kern, *Nano Letters*, 2007, **7**, 3499-3503 (DOI:10.1021/nl072090c)
- Y. Harima, S. Setodoi, I. Imae, K. Komaguchi, Y. Ooyama, J. Ohshita, H. Mizota and J. Yan, *Electrochim. Acta*, 2011, **56**, 5363-5368 (DOI:10.1016/j.electacta.2011.03.117)
- W. Li, J. Liu and C. Yan, *Carbon*, 2013, **55**, 313-320 (DOI:10.1016/j.carbon.2012.12.069)
- C. Kvarnstrom, H. Neugebauer and A. Ivaska, in *Advanced Functional Molecules and Polymers*, ed. ed. H. S. Nalwa, Gordon and Breach Publishers, Amsterdam, 2001, pp.139.
- A. Osterholm, P. Damlin, C. Kvarnstrom and A. Ivaska, *Physical Chemistry Chemical Physics*, 2011, **13**, 11254-11263 (DOI:10.1039/c1cp20246d)
- A. Viinikanoja, Z. Wang, J. Kauppila and C. Kvarnstrom, *Physical Chemistry Chemical Physics*, 2012, **14**, 14003-14009 (DOI:10.1039/c2cp42253k)
- M. Hirata, T. Gotou, S. Horiuchi, M. Fujiwara and M. Ohba, *Carbon*, 2004, **42**, 2929-2937 (DOI:10.1016/j.carbon.2004.07.003)
- P. Gao, D. Gosztola, L. W. H. Leung and M. J. Weaver, *J Electroanal Chem*, 1987, **233**, 211-222 (DOI:10.1016/0022-0728(87)85017-9)
- P. Damlin, C. Kvarnstrom, A. Petr, P. Ek, L. Dunsch and A. Ivaska, *Journal of Solid State Electrochemistry*, 2002, **6**, 291-301 (DOI:10.1007/s100080100240)
- S. Park and R. S. Ruoff, *Nature Nanotechnology*, 2009, **4**, 217-224 (DOI:10.1038/NNANO.2009.58)
- G. K. Ramesha and S. Sampath, *Journal of Physical Chemistry C*, 2009, **113**, 7985-7989 (DOI:10.1021/jp811377n)
- A. Y. S. Eng, A. Ambrosi, C. K. Chua, F. Sanek, Z. Sofer and M. Pumera, *Chemistry-a European Journal*, 2013, **19**, 12673-12683 (DOI:10.1002/chem.201301889)
- K. Boujlel and J. Simonet, *Electrochim. Acta*, 1979, **24**, 481-487 (DOI:10.1016/0013-4686(79)85020-3)
- Z. Wang, X. Zhou, J. Zhang, F. Boey and H. Zhang, *Journal of Physical Chemistry C*, 2009, **113**, 14071-14075 (DOI:10.1021/jp906348x)
- A. Bonanni, A. Ambrosi and M. Pumera, *Chemistry-a European Journal*, 2012, **18**, 1668-1673 (DOI:10.1002/chem.201102850)
- Kretschm.E and H. Raether, *Zeitschrift Fur Naturforschung Part A-Astrophysik Physik Und Physikalische Chemie*, 1968, **A 23**, 2135-&
- C. Hontorialucas, A. J. Lopezpeinado, J. D. D. Lopezgonzalez, M. L. Rojascervantes and R. M. Martinaranda, *Carbon*, 1995, **33**, 1585-1592 (DOI:10.1016/0008-6223(95)00120-3)
- M. Acik, G. Lee, C. Mattevi, A. Pirkle, R. M. Wallace, M. Chhowalla, K. Cho and Y. Chabal, *Journal of Physical Chemistry C*, 2011, **115**, 19761-19781 (DOI:10.1021/jp2052618)
- H. Lund, in *Organic Electrochemistry*, ed. ed. H. Lund and O. Hammerich, Marcel Dekker, Inc., New York, 2001, pp.270.
- A. C. Ferrari, J. C. Meyer, V. Scardaci, C. Casiraghi, M. Lazzeri, F. Mauri, S. Piscanec, D. Jiang, K. S. Novoselov, S. Roth and A. K. Geim, *Phys. Rev. Lett.*, 2006, **97**, 187401 (DOI:10.1103/PhysRevLett.97.187401)
- M. R. Baldan, E. C. Almeida, A. F. Azevedo, E. S. Goncalves, M. C. Rezende and N. G. Ferreira, *Appl. Surf. Sci.*, 2007, **254**, 600-603 (DOI:10.1016/j.apsusc.2007.06.038)
- C. Thomsen and S. Reich, *Phys. Rev. Lett.*, 2000, **85**, 5214-5217 (DOI:10.1103/PhysRevLett.85.5214)
- M. M. Lucchese, F. Stavale, E. H. M. Ferreira, C. Vilani, M. V. O. Moutinho, R. B. Capaz, C. A. Achete and A. Jorio, *Carbon*, 2010, **48**, 1592-1597 (DOI:10.1016/j.carbon.2009.12.057)
- F. Tuinstra and J. L. Koenig, *J. Chem. Phys.*, 1970, **53**, 1126-& (DOI:10.1063/1.1674108)
- R. Vidano and D. B. Fischbach, *J Am Ceram Soc*, 1978, **61**, 13-17 (DOI:10.1111/j.1151-2916.1978.tb09219.x)
- M. Bousa, O. Frank and L. Kavan, *Electroanalysis*, 2014, **26**, 57-61 (DOI:10.1002/elan.201300340)
- A. C. Ferrari and J. Robertson, *Physical Review B*, 2000, **61**, 14095-14107 (DOI:10.1103/PhysRevB.61.14095)
- L. G. Cancado, A. Jorio, E. H. Martins Ferreira, F. Stavale, C. A. Achete, R. B. Capaz, M. V. O. Moutinho, A. Lombardo, T. S. Kulmala and A. C. Ferrari, *Nano Letters*, 2011, **11**, 3190-3196 (DOI:10.1021/nl201432g)
- M. Bousa, O. Frank, I. Jirka and L. Kavan, *Physica Status Solidi B-Basic Solid State Physics*, 2013, **250**, 2662-2667 (DOI:10.1002/pssb.201300105)